Anisotropic Crystalline Organic Step-Flow Growth on Deactivated Si Surfaces

Sean R. Wagner, Richard R. Lunt, and Pengpeng Zhang

Phys. Rev. Lett. **110**, 086107 — Published 20 February 2013

DOI: 10.1103/PhysRevLett.110.086107

Anisotropic Crystalline Organic Step-Flow Growth on Deactivated Si Surfaces

Sean R. Wagner,[1] Richard R. Lunt,[2] and Pengpeng Zhang[1,*]

[1] *Department of Physics and Astronomy, Michigan State University, East Lansing, Michigan 48824-2320, USA*
[2] *Department of Chemical Engineering and Materials Science, Michigan State University, East Lansing, Michigan 48824-2320, USA*

We report the first demonstration of anisotropic step-flow growth of organic molecules on a semiconducting substrate using metal phthalocyanine thermally deposited on the deactivated Si(111)-B $\sqrt{3} \times \sqrt{3}$ $R30^\circ$ surface. With scanning probe microscopy (SPM) and geometric modeling, we prove the quasi-epitaxial nature of this step-flow growth that exhibits no true commensurism, despite a single dominant long-range ordered relationship between the organic crystalline film and the substrate, uniquely distinct from inorganic epitaxial growth. This growth mode can likely be generalized for a range of organic molecules on deactivated Si surfaces and access to it offers new potential for the integration of ordered organic thin films in silicon-based electronics.

PACS numbers: 68.55.am, 68.43.Hn, 68.37.Ef, 68.35.bm

Control of highly ordered organic molecular thin films with extended π systems is currently of intense interest for integration into modern electronics due to the tunable nature of organic molecules [1, 2]. Selection of molecules and substrate can lead to desired transport properties such as charge transfer, charge injection, exciton diffusion, etc., at the hybrid hetero-interface, which is central to the development of organic and molecular electronics [3–7]. However, achieving large-scale molecular ordering remains a significant challenge. Strong molecule-substrate interaction can hinder molecular diffusion and organization on the surface, while strong molecule-molecule interaction results in island growth and the formation of polycrystalline or polymorphic films [8, 9]. Therefore, it is desirable to tip the balance between molecule-molecule and molecule-substrate interactions, and to grow organic thin films that are ordered in both the perpendicular and in-plane directions [10].

Recently, intense efforts have been devoted to achieve in-plane azimuthal ordering in organic thin films by depositing molecules on low symmetry surfaces [11, 12] or on vicinal substrates [13–19]. The high anisotropy nature of low symmetry substrates can effectively suppress rotated molecular domains while vicinal substrates can lead to preferential binding of molecules at step-edges [17, 20]. Nevertheless, growth on vicinal metal substrates often results in the coexistence of a short-ranged in-plane azimuthal-ordered "step phase" and a polycrystalline "terrace phase" because of the strong molecule-substrate interaction that can exhibit covalent bonding character and impedes diffusion of molecules on the surface [20–22]. Additionally, this covalent bonding typically drives commensurate molecular registry and forces molecules to deviate from the bulk phase; this typically leads to molecular relaxation within a few monolayers and the formation of amorphous, two-dimensional or three-dimensional powder growth. Alternatively, substrates such as SiO_2 with weak interactions have proven unable to support long-range in-plane crystallization across a substrate since domains are generally randomly oriented [23] resulting in high-angle grain boundaries that can efficiently scatter or trap carriers in the charge transport [24, 25]. Therefore, it is important to find routes to guide the long-range ordered organic growth on a large-scale in all directions.

In this study we report the quasi-epitaxial growth of zinc phthalocyanine (ZnPc), an archetypal molecule with demonstrated applications in organic electronics [26, 27] and photovoltaics [1, 28], on an atomically flat and deactivated Si(111)-B surface. In addition to the formation of Moiré patterns characteristic of the quasi-epitaxial (non-commensurate) growth, we find that ZnPc molecules diffuse rapidly on the surface to nucleate at Si step-edges followed by the formation of highly ordered anisotropic structures across Si terraces, i.e. step-flow growth. The step-flow growth mode further impacts the quasi-epitaxial nature of the growth by reducing the effective substrate symmetry and allowing for the formation of thin films with an exclusive in-plane azimuthal relationship. Our results indicate that the interaction between ZnPc and the substrate is sufficiently weak to allow the molecules to diffuse across μm-wide terraces at room temperature, but sufficiently strong to induce in-plane azimuthal ordering and quasi-epitaxial growth. The temperature dependence of this novel growth regime is mapped for both CuPc and ZnPc, and a microscopic mechanism is discussed which suggests that step-flow growth on deactivated Si(111)-B can be extended to a large variety of organic systems.

The Si(111)-B $\sqrt{3} \times \sqrt{3}$ $R30^\circ$ surface was prepared from a heavily boron doped Si(111) wafer. The substrate was first cleaned *ex-situ* by the standard semiconductor RCA1 and RCA2 procedures, leaving a thin (1-2 nm) surface oxide. The sample was transported to the preparation chamber of the Omicron ultra-high vacuum (UHV) low temperature scanning tunneling microscope maintained at a pressure below 1.0×10^{-10}mB. *In-situ*, the surface was annealed at 1200 °C by direct current heating to remove the oxide layer, followed by an hour of annealing at 800 °C to induce boron segregation. ZnPc films were grown at room temperature by thermal evaporation from a boron nitride crucible with a typical chamber pressure of $\sim 8.0 \times 10^{-10}$mB during deposition. After deposition, samples were transferred *in-situ* to the LT-STM chamber and cooled to 77K for scanning tunneling microscopy (STM) and scanning tunneling spectroscopy (STS) measurements. STS spectra and differential conductance images were obtained by detecting AC tunneling current through a lock-in amplifier with the sample bias modulated by a 750 Hz signal at an amplitude of 30 mV. We carried out AFM experiments using an Asylum Research MFP-3D atomic force microscope on freshly deposited ZnPc thin films which were transferred from the UHV system to a nitrogen flow cell to minimize exposure to air.

A deactivated Si(111)-B surface is formed when B atoms diffuse into the third atomic layer and deplete charge from the dangling bonds of the topmost Si adatoms [29–31]. A typical STM image of the deactivated Si surface is shown in Fig. 1(a). This deactivated and atomically flat Si surface provides a unique substrate to form large-scale highly-ordered organic thin films, as demonstrated in Fig. 1(b) where ZnPc molecules crystallize in azimuthally ordered form with a periodic structure. Furthermore, a two-dimensional (2D) Moiré pattern formation can be observed by the bright features in Fig. 1(b), suggesting that the molecular overlayer is not commensurate with the substrate and only specific molecules come close to registering with Si adatoms to yield the enhanced electronic density of states [32].

To determine the epitaxial relation between the molecular overlayer and the Si substrate, we conducted STM

experiments on a Si surface that is partially covered by ZnPc structures. We first carried out STS on both the Si surface and the ZnPc molecules to identify the sample bias to use for imaging the molecules. Fig. 2(a) shows the spectra taken on Si adatoms and on ZnPc, respectively. The Si spectrum reveals that the surface has been deactivated with the unoccupied state at about 1.5 eV above the Fermi level and an occupied back-bond state at about 1.5 eV below the Fermi level, consistent with the previous study [31]. Spectrum on ZnPc shows the available density of states near +2.5 V, corresponding to the resonant tunneling through the lowest unoccupied molecular orbital (LUMO) [33, 34].

Due to the convolution between topology and density of states inherent in STM imaging we additionally performed simultaneous differential conductance map measurements to assign the orientation of deposited ZnPc molecules. Fig. 2(b) shows that only 2 of the benzene rings in the ZnPc structure are resolved per molecule, as represented by the black lines, implying a tilted molecular orientation. We calculated the LUMO of free ZnPc molecules in this tilted orientation using density functio-

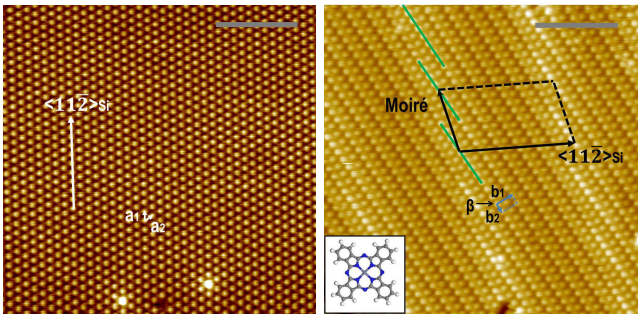

(a) (b)

FIG. 1. (a) STM topography image (V_s=+2 V, I_t=150 pA) of the deactivated Si(111)-B surface obtained at 77K. Surface is hexagonal with lattice parameter $a = 6.65 \pm 0.05$Å. Bright features correspond to Si dangling bonds with the absence of underlying boron atoms. An individual adatom vacancy can also be observed. (b) STM topography image (V_s=+2 V, I_t=35 pA) of ZnPc on deactivated Si(111)-B obtained at 77K. Unit cell of the molecular overlayer given by: $b_1 = 12.3 \pm 0.1$Å, $b_2 = 6.7 \pm 0.1$Å, and $\beta = 92 \pm 1\,^\circ$. Green lines mark bright fringes of the Moiré pattern. The periodicity of the pattern is 8.3 ± 0.2nm along the $\langle 11\overline{2} \rangle$ direction of the Si substrate and 5.0 ± 0.2nm along the Moiré direction with angle of $104 \pm 2\,^\circ$ between the two, highlighted by black arrows. The gray scale bars are 6 nm (inset: atomic model of the ZnPc molecule).

nal theory, which is in agreement with the electron density distribution of molecular orbitals observed in the differential conductance map. Next we focus our discussion on the epitaxial relation between the ZnPc overlayer and the Si substrate. As illustrated in Fig. 2(b), the smallest unit cell of the molecular overlayer is rotated by $27 \pm 2\,^\circ$ from the $\langle 11\overline{2} \rangle$ direction of Si(111)-B surface. This well-defined azimuthal orientation is the key characteristic of the organic quasi-epitaxial growth. Furthermore, we find that both the lateral unit cell and the d-spacing [35] of the deposited ZnPc overlayers on the deactivated Si surface are distorted from the bulk phase [36], despite the lack of formation of a commensurate structure.Rather, the initial nucleation events are guided by the equilibrium minimum in the energetic landscape that appears nearly point-on-line (POL) coincident for small domains but becomes more incommensurate for complete layers.

The observation of Moiré pattern and the quasi-epitaxial relation of the ZnPc molecular overlayer on the Si substrate can be quantitatively interpreted by calculations using the geometric phase coherence model which have already shown success in determining epitaxial configurations in many organic systems [32]. In this calculation the periodicity of the substrate lattice and molecular overlayer lattice are represented as plane waves that correspond to an idealized surface potential. We determine the discrete ratio of the plane wave potentials with the overlayer rotated azimuthally with respect to the substrate which correlates to the epitaxial relation. The structure transformation matrix is given by:

$$\begin{bmatrix} \frac{b_1 sin(\alpha-\theta)}{a_1 sin(\alpha)} & \frac{b_1 sin(\theta)}{a_2 sin(\alpha)} \\ \frac{b_2 sin(\alpha-\theta-\beta)}{a_1 sin(\alpha)} & \frac{b_2 sin(\theta+\beta)}{a_2 sin(\alpha)} \end{bmatrix} = \begin{bmatrix} M_{11} & M_{12} \\ M_{21} & M_{22} \end{bmatrix} \quad (1)$$

where a_1, a_2, and α are the substrate lattice parameters, b_1, b_2, and β are the molecular overlayer lattice parameters,

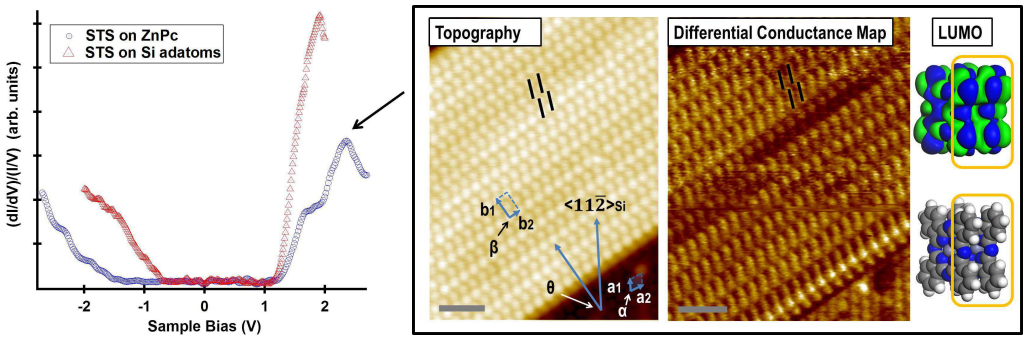

(a) (b)

FIG. 2. (a) Normalized STS spectra taken on the deactivated Si adatom sites (red) and ZnPc molecules (blue) over the same area as shown in (b). The peak in the ZnPc spectra near +2.5V was used for the simultaneous imaging of topology and differential conductance map in (b). (b) Left: Partial image showing both the ZnPc overlayer and the Si surface (I_t=50 pA, 77K). θ represents the angle between a_1 and b_1, defining the azimuthal relation between the molecular overlayer and the substrate. Right: Differential conductance map taken simultaneously at the same imaging conditions. Black lines represent individual molecules with edge-to-edge distance between the 2 benzene rings measured to be 13.0 ± 0.2Å. Inset: atomic model of a ZnPc dimer in observed tilted orientation and LUMO of free ZnPc molecules calculated using density functional theory and the Perdew-Wang generalized gradient approximation. Gray scale bars are 3 nm.

and θ is the azimuthal angle. V/V_0 is defined by the following:

$$V/V_0 = \left(\frac{1}{2N^2}\right)\left[2N^2 - \frac{\sin(\pi N M_{11})\sin(\pi N M_{21})}{\sin(\pi M_{11})\sin(\pi M_{21})} - \frac{\sin(\pi N M_{12})\sin(\pi N M_{22})}{\sin(\pi M_{12})\sin(\pi M_{22})}\right] \tag{2}$$

where N is related to the size of the molecular overlayer [32]. After substituting in the lattice parameters (a_1, a_2, α, b_1, b_2, β) determined from experiment, V/V_0 is then varied with respect to θ to find minima for V/V_0. A ratio of $V/V_0 = 1$, $V/V_0 = 0.5$, and $V/V_0 = 0$ correspond to incommensurate, POL coincidence, and commensurate relationships, respectively. As shown in Fig. 3(a), we found that an azimuthal rotation of $28 \pm 0.5\,^\circ$ gives a minimum value of $V/V_0 \sim 0.7$, which indicates a quasi-epitaxial relation between incommensurate and POL coincidence. Other minima in the model occur at $60\,^\circ$ intervals consistent with the substrate C3 symmetry. Using the calculated azimuthal angle and the experimentally determined lattice parameters, a simulated image of the ZnPc molecular overlayer on the deactivated Si surface (Fig. 3(b)) was generated. Analysis of the simulated and STM Moiré patterns (which are highly sensitive to this azimuthal relationship) are in excellent agreement, with the periodicity of the fringe pattern (green lines in Fig. 1(b) and 3(b)) and the angle of the Moiré fringes with respect to the $\langle 11\bar{2} \rangle$ direction of the Si(111)-B surface both within the measured error.

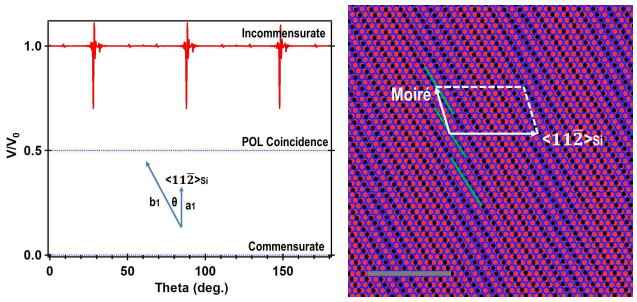

(a) (b)

FIG. 3. (a) Results of a geometric analysis as the molecular overlayer is rotated azimuthally on the Si substrate. First minimum in V/V_0 ($= 0.7$) occurs at $28 \pm 0.5\,^\circ$ with other minima spaced in increments of $60\,^\circ$ due to the substrate C3 symmetry. (b) Simulated overlayer-substrate geometry at an azimuthal rotation angle of $28\,^\circ$. Red circles outlined in blue represent Si adatoms. Black dots represent the ZnPc overlayer lattice. Green lines mark the bright fringes of the Moiré pattern. The periodicity of the pattern is 8.5 ± 0.1nm along the $\langle 11\overline{2} \rangle$ direction of the Si substrate and 4.8 ± 0.1nm along the Moiré direction with angle of $104 \pm 1\,^\circ$ between the two, highlighted by white arrows for comparison with Figure 1(b). Gray scale bar is 8 nm.

In principle, the growth of molecular species on a surface is determined by the competition between thermodynamics and kinetics [37]. If the deposition rate is slower than the diffusion rate, the growth of molecular structures occurs close to thermal equilibrium conditions. Step-flow growth is generally observed in inorganic epitaxial growth when the nucleation of deposited species is energetically favored at step-edges and the diffusion length is long enough to enable such site sampling prior to flux accumulation on the terrace [38, 39]. The controlled crystalline growth of organic semiconductors has been of longstanding interest in the attempt to find analogous growth modes to inorganic semiconductor deposition [40–42]. As shown in Fig. 4(a), we demonstrated evidence of the step-flow growth mode of Pc molecules starting from the first monolayer on a solid surface. ZnPc molecules rapidly diffuse on the Si(111)-B surface and preferentially nucleate at the step-edges, a phenomenon uniformly observed across the substrate. However, the anisotropy of this growth distinguishes it from inorganic step-flow growth. Once the step-edge sites are occupied, stripe structures expand across the terraces until they reach the next step-edge (without the presence of intra-terrace nucleation). The anisotropic growth of stripe structures is attributed to the favored π stacking between molecules, where the exposed surfaces are likely the lowest energy surfaces of the crystal structure, analogous to other Pc systems. Upon reaching the next step-edge, stripes proceed to grow in the in-plane perpendicular direction, widening until the stripes coalesce to complete a monolayer. It is known that molecules are often impacted by Ehrlich-Schwöebel barriers (ESB) that originate from the loss of atomic coordination at self- or heterointerface step-edges [43]. Our observations during the growth of the first monolayer suggest that an ESB associated with downward molecular transport across the Si step-edges is likely present, while the ESB for edge-crossing of ZnPc molecular stripes is negligible at room temperature.

The formation of aligned structures due to the anisotropic growth persists even with growth beyond the first layer. Fig. 4(b) shows an AFM topology on a sample with a complete first monolayer and partial second and third layers. We can clearly see that the majority of the second and third monolayers continue to display the same anisotropic step-flow growth as the first monolayer, where the location of Si steps can be clearly identified even after the growth up to 3 organic layers. Although three different orientations of the ZnPc stripe structures are observed at various defect sites, consistent with the C3 symmetry of the substrate, the growth is almost entirely dominated by a singular orientation that provides the shortest path between step-edges. This phenomenon is highly desirable since the formation of low-angle twin boundaries of the adjacent stripe structures is preferred over randomly orientated boundaries (often observed during the island growth) for achieving superior in-plane electrical and excitonic transport [24, 25]. Furthermore, such a step-flow growth of molecules on the Si(111)-B deactivated surface may allow for macroscopic ordered structures to form on vicinal substrates with an even lower miscut.

Lastly, we offer a physical interpretation for the growth of ZnPc on the deactivated Si(111)-B surface. We attribute the step-flow growth mode to the large diffusivity of ZnPc molecules and the low defect density of the Si(111)-B surface which efficiently suppresses the island

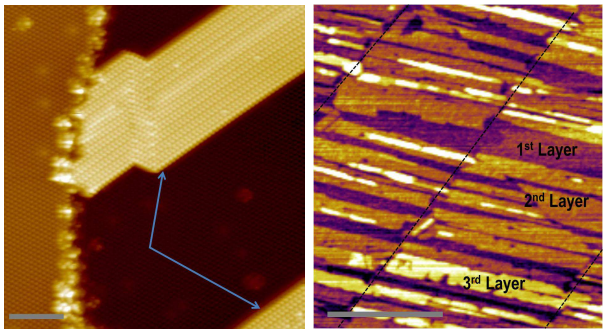

(a) (b)

FIG. 4. (a) STM topography image (V_s=+2 V, I_t=30 pA) showing the initial step flow growth of ZnPc on Si(111)-B. Two parallel molecular stripes (arrows) originating from the same Si step are observed. Gray scale bar is 8 nm. (b) Tapping mode AFM topography image (with AC240TM cantilevers from Asylum Research, k=2 N/m, f_0=70 kHz) of ZnPc thin film growth on Si(111)-B surface with a complete first monolayer and partial second/third layer coverage. Anisotropic step flow growth is observed for both the second and third monolayers with a dominant orientation with respect to the Si steps. The gray scale bar is 500 nm.

nucleation on terraces and allows molecules to fully explore the surface at room temperature to find preferential nucleation sites at the steps (see Supplemental Section for temperature dependence of the growth mode and detailed theoretical nucleation rate considerations [35]). There are several factors contributing to the large diffusivity of ZnPc molecules: (i) The Si(111)-B surface is deactivated without any density of states present at the Fermi level, leading to a relatively weak molecule-substrate interaction and the non-commensurate molecular registration to the substrate; (ii) The geometric parameters of the molecule, including its size and symmetry, do not match with the substrate. As a consequence, the effective corrugation of the substrate surface potential is smeared out over the size of the molecule, which effectively reduces the activation barrier for diffusion. It is worth noting that we also observed similar characteristics on the CuPc growth (see Supplemental Section [35]), and we speculate that this growth mode can be extended to other organic molecules on the deactivated Si surface provided that the above scenarios are met. The step-flow growth mode further impacts the quasi-epitaxial nature of the growth by reducing the effective substrate symmetry and allowing for the formation of aligned heterostructured crystalline thin films, which offer the potential for improved performance for OFETs and nanowire/nanoribbon devices.

This research is funded by the U. S. Department of Energy (DOE) Office of Science Early Career Research Program (Grant number DE-SC0006400) through the Office of Basic Energy Sciences. We also acknowledge the start-up support from Michigan State University. We thank Jiebing Sun for his help on the AFM experiments.

* zhang@pa.msu.edu

[1] F. Yang, M. Shtein, and S. R. Forrest, *Nat. Mater.*, **4**, 37 (2005).
[2] G. Witte and C. Wöll, *J. Mater. Res.*, **19**, 1889 (2004).
[3] J. Hwang, A. Wan, and A. Kahn, *Mat. Sci. Eng. R*, **64**, 1 (2009).
[4] S. Duhm, G. Heimel, I. Salzmann, H. Glowatzki, R. L. Johnson, A. Vollmer, J. P. Rabe, and N. Koch, *Nat. Mater.*, **7**, 326 (2008).
[5] R. R. Lunt, J. B. Benziger, and S. R. Forrest, *Adv. Mater.*, **22**, 1233 (2010).
[6] D. J. Michalak, S. R. Amy, D. Aureau, M. Dai, A. Estéve, and Y. J. Chabal, *Nat. Mater.*, **9**, 266 (2010).
[7] B. Lee, Y. Chen, F. Duerr, D. Mastrogiovanni, E. Garfunkel, E. Y. Andrei, and V. Podzorov, *Nano Lett.*, **10**, 2427 (2010).
[8] J. V. Barth, *Annu. Rev. Phys. Chem.*, **55**, 375 (2007).
[9] J. Götzen, D. Käfer, C. Wöll, and G. Witte, *Phys. Rev. B*, **81**, 085440 (2010).
[10] G. E. Thayer, J. T. Sadowski, F. Meyer zu Heringdorf, T. Sakurai, and R. M. Tromp, *Phys. Rev. Lett.*, **95**, 256106 (2005).
[11] G. Koller, S. Berkebile, J. R. Krenn, G. Tzvetkov, G. Hlawacek, O. Lengyel, F. P. Netzer, C. Teichert, R. Resel, and M. G. Ramsey, *Adv. Mater.*, **16**, 2159 (2004).
[12] L. Sun, G. Weidlinger, M. Denk, R. Denk, M. Hohage, and P. Zeppenfeld, *Phys. Chem. Chem. Phys.*, **12**, 14706 (2010).
[13] J. Götzen, S. Lukas, A. Birkner, G. Witte, *Surf. Sci.*, **605**, 577 (2011).
[14] T. Shimada, M. Ohtomo, T. Suzuki, T. Hasegawa, and K. Ueno, *Appl. Phys. Lett.*, **93**, 223303 (2008).
[15] S. Lukas, S. Vollmer, G. Witte, and Ch. Wöll, *J. Chem. Phys.*, **114**, 10123 (2001).
[16] V. Ignatescu, J.-C. M. Hsu, A. C. Mayer, J. M. Blakely, and G. G. Malliaras, *Appl. Phys. Lett.*, **89**, 253116 (2006).
[17] M. Eremtchenko, R. Temirov, D. Bauer, J. A. Schaefer, and F. S. Tautz, *Phys. Rev. B*, **72**, 115430 (2005).
[18] E. Barrena, J. O. Ossó, F. Schreiber, M. Garriga, M. I. Alonso, and H. Dosch, *J. Mater. Res.*, **19**, 2061 (2004).
[19] J. O. Ossó, F. Schreiber, V. Kruppa, H. Dosch, M. Garriga, M. I. Alonso, and F. Cerdeira, *Adv. Funct. Mater.*, **12**, 455 (2002).
[20] H. Glowatzki, S. Duhm, K.-F. Braun, J. P. Rabe, and N. Koch, *Phys. Rev. B*, **76**, 125425 (2007).
[21] Y. Wakayama, *J. Phys. Chem. C*, **111**, 2675 (2007).
[22] D. G. de Oteyza, E. Barrena, H. Dosch, and Y. Wakayama, *Phys. Chem. Chem. Phys.*, **11**, 8741 (2009).
[23] R. R. Lunt, J. B. Benziger, and S. R. Forrest, *Appl. Phys. Lett.*, **90**, 181932 (2007).
[24] J. Rivnay, L. H. Jimison, J. E. Northrup, M. F. Toney, R. Noriega, S. Lu, T. J. Marks, A. Facchetti, and A. Salleo, *Nat. Mater.*, **8**, 952 (2009).
[25] A. B. Chwang and C. D. Frisbie, *J. Appl. Phys.*, **90**, 1342 (2001).
[26] S. A. Van Slyke, C. H. Chen, and C. W. Tang, *Appl. Phys. Lett.*, **69**, 2160 (1996).
[27] Z. Bao, A. J. Lovinger, and J. Brown, *J. Am. Chem. Soc.*, **120**, 207 (1998).
[28] D. Y. Kim, F. So, and Y. Gao, *Sol. Energ. Mat. Sol. Cells*, **93**, 1688 (2009).
[29] Y. Makoudi, F. Palmino, M. Arab, E. Duverger, and F. Chérioux, *J. Am. Chem. Soc.*, **130**, 6670 (2008).
[30] B. Baris, V. Luzet, E. Duverger, P. Sonnet, F. Palmino, and F. Chérioux, *Angew. Chem. Int. Ed.*, **50**, 4094 (2011).
[31] I.-W. Lyo, E. Kaxiras, and Ph. Avouris, *Phys. Rev. Lett.*, **63**, 1261 (1989).
[32] D. E. Hooks, T. Fritz, and M. D. Ward, *Adv. Mater.*, **13**, 227 (2001).
[33] K. W. Hipps, D. E. Barlow, and U. Mazur, *J. Phys. Chem. B*, **104**, 2444 (2000).
[34] M. Lackinger, T. Muller, T. G. Gopakumar, F. Muller, M. Hietschold, and G. W. Flynn, *J. Phys. Chem. B*, **108**, 2279 (2004).
[35] See Supplemental Material at (insert link here) for supplementary figures.
[36] T. Kobayashi, Y. Fujiyoshi, F. Iwatsu, and N. Uyeda, *Acta Cryst.*, **A37**, 692 (1981).
[37] T. V. Desai, A. R. Woll, F. Scheiber, and J. R. Engstrom, *J. Phys. Chem. C*, **114**, 20120 (2010).
[38] M. H. Xie, S. M. Seutter, W. K. Zhu, L. X. Zheng, H. Wu, and S. Y. Tong, *Phys. Rev. Lett.*, **82**, 2749 (1999).
[39] L. Bai, J. Tersoff, and F. Liu, *Phys. Rev. Lett.*, **92**, 225503 (2004).
[40] F.-J. Meyer zu Heringdorf, M. C. Reuter, and R. M. Tromp, *Nature*, **412**, 517 (2001).
[41] M. B. Casu, S.-A. Savu, B.-E. Schuster, I. Biswas, C. Raisch, H. Marchetto, Th. Schmidt, and T. Chassé, *Chem. Commun.*, **48**, 6957 (2012).
[42] S. Verlaak, S. Steudel, P. Heremans, D. Janssen, and M. S. Deleuze, *Phys. Rev. B*, **68**, 195409 (2003).
[43] J. E. Goose, E. L. First, and P. Clancy, *Phys. Rev. B*, **81**, 205310 (2010).